



Research Article

Algebraic Method for Approximate Solution of Scattering of Surface Waves by Thin Vertical Barrier Over a Stepped Bottom Topography

Naveen Kumar^{1,2} , Deepali Goyal¹, S. C. Martha^{1*} 

¹Department of Mathematics, Indian Institute of Technology Ropar, Rupnagar-140001, Punjab, India

²Government College Krishan Nagar, Mahendergarh-123001, Haryana, India

E-mail: scmartha@iitrpr.ac.in, scmartha@gmail.com

Received: 18 July 2022; **Revised:** 10 October 2022; **Accepted:** 25 October 2022

Abstract: A study on interaction of surface water waves by thin vertical rigid barrier over a step type bottom topography is analysed. The associated mixed boundary value problem is solved using the eigenfunction expansion of the velocity potential. The resulting system of equations, avoiding the traditional approach of employing application of orthogonality relations, is solved using algebraic least squares method giving rise the numerical values of the reflection and transmission coefficients by the barrier over step. The energy balance relation for the given problem is derived and verified numerically ensuring the correctness of the present results. The present results are also compared with the data available in the literature for the validation purpose. The effect of step height, length of the barrier and angle of incidence on the reflection coefficient and the non-dimensional horizontal force on the barrier have been investigated through different plots. It is observed that barrier along with step works as an effective barrier to reflect more incident waves causing calm zone along the leeside.

Keywords: scattering of waves, eigenfunction expansion, least-squares method, reflection and transmission coefficients, force on the barrier over step

MSC: 76B15

1. Introduction

Over the years, many researchers are drawing great attention to the study of problems involving propagation of water waves in the presence of barrier over uniform finite depth of water due to their applications in ocean engineering to create tranquillity zones by reflecting and dissipating maximum incident wave energy to ensure the safety of coastal structures like ports, bays and harbours. For this purpose either floating or submerged breakwaters are usually installed in the coastal area worldwide. In this context, the problems of diffraction of obliquely incident water waves by a vertical plate, a horizontal plate and rectangular cylinder are studied using finite element technique by Bai [1]. The finite element method was used to represent the velocity potential where the variation principle was used to determine the unknowns such as reflection and transmission coefficients and the diffraction forces and moments. Evans [2] studied the diffraction of water waves by a submerged thin vertical plate where the linearized boundary value problem was solved in closed form for the velocity potential everywhere in the fluid and on the plate. The expressions for the first-order and second-

Copyright ©2022 S. C. Martha, et al.

DOI: <https://doi.org/10.37256/cm.3420221711>

This is an open-access article distributed under a CC BY license
(Creative Commons Attribution 4.0 International License)

<https://creativecommons.org/licenses/by/4.0/>

order forces and moments on the plate are also derived. An eigenfunction expansion method was used to investigate the scattering of obliquely incident surface waves by thin vertical barrier with three different configurations namely descending from the free surface, bottom standing and submerged slit by Losada et al. [3]. A method of approximation based on Galerkin approximation was used to analyse the scattering of oblique incident water waves by a vertical barrier in finite depth of the water by Porter [4] where the zeros of reflection and transmission curves against the spacing between the barriers were also investigated. Gayen and Mondal [5] studied wave scattering by a thin inclined porous plate by using hypersingular integral equation approach.

Often the ocean floor is rough rather than uniform. This makes, it significant to consider the problems of propagation of water waves over an uneven sea bed, which are also interesting due to their importance in coastal and marine engineering. The problem of water wave scattering by a rectangular submarine trench was analyzed assuming linearized theory of water waves by Chakraborty and Mandal [6-7], where the boundary value problem was split into two separate problems involving the symmetric and antisymmetric potential functions and the reflection and transmission coefficients were calculated using a multi-term Galerkin approximation involving ultra-spherical Gegenbauer polynomials. Further, the problem of surface-piercing structures and the bottom profiles, where the bottom profiles were sliced into shelves separated by abrupt steps, was investigated by Tseng [8]. For each shelf, the Bragg reflection of oblique waves was analyzed using the eigenfunction matching method based on small amplitude wave theory. Tran et al. [9] investigated the scattering of oblique water waves by multiple thin barriers over undulated bottom using matched eigenfunction expansion method after slicing the bottom topography into shelves separated by steps. Borah and Hassan [10] studied the problem of diffraction of water waves by partially submerged floating hollow cylinder placed over a fixed coaxial bottom-mounted obstacle and solved it with the help of matched eigenfunction expansion to obtain analytical expressions of potentials. Koley et al. [11] investigated the oblique wave trapping by bottom-standing and surface-piercing porous structures of finite width placed at a finite distance from a vertical rigid wall using the Sollitt and Cross Model. Panduranga et al. [12] investigated the effectiveness of multiple slatted screens placed in front of a caissons porous breakwater in the presence of seabed undulation to dissipate the incident wave energy using an iterative multi-domain boundary element method. In a similar manner, the problem involving step type bottom topographies was also studied by many researchers by different methods. Das and Bora [13] studied the reflection of oblique ocean water waves by a vertical porous structure placed on an elevated impermeable seabed consisting of a number of horizontal steps by employing the matched eigenfunction expansion method. The impact of a porous rectangular barrier placed over the seabed with the dynamic characteristics of gravity waves was analyzed by Meng and Lu [14] by employing the method of matched eigenfunction expansions. A problem of oblique interaction between water waves and a partially submerged rectangular floating breakwater in water of uneven depth was analyzed by Kaligatla et al. [15] whereas the problem of water wave propagation over a rectangular submarine trench in the presence of a thin vertical partially immersed barrier was investigated by employing Galerkin approximation method by Ray et al. [16]. Liu et al. [17] constructed an analytical solution in terms of Taylor series to the modified mild-slope equation (MMSE) for surface waves propagating over a finite array of trapezoidal artificial bars from deep water to shallow water. The study of water waves propagating over a permeable sea bottom was constructed using MMSE by Ni and Teng [18]. Singh et al. [19] and Singh et al. [20] studied the reflection of plane waves at the stress-free/rigid surface of a micro-mechanically modeled piezo-electro-magnetic fiber-reinforced composite half-space. A study on the head-on collision between two solitary waves in a thin elastic plate floating on an inviscid fluid of finite depth was examined analytically by means of a singular perturbation method by Bhatti and Lu [21]. An analytical study for oblique wave interaction with a semi-infinite elastic plate with finite draft over a step bottom topography was examined using matched eigenfunction expansions by Guo et al. [22] by incorporating three different plate edge conditions namely free, simply supported and built-in conditions. Venkateswarlu and Karmakar [23] analyzed wave scattering due to multiple porous structures over an impermeable elevated bottom. Dhillon et al. [24] investigated the water wave scattering by a dock of finite width over a step-type bottom topography using expansion formula for velocity potential. Praveen et al. [25] investigated wave transformation due to finite elastic dock over abrupt change in bottom topography. Vijay et al. [26] studied Bragg scattering of surface wave train by an array of submerged breakwater and a floating dock. Guha and Singh [28] studied reflection/transmission of plane waves in an initially stressed rotating piezo-electro-magnetic fiber-reinforced composite half-space.

Keeping in view of the above works, vertical barrier over a stepped bottom will be an interesting addition towards

an effective barrier. Hence, the aim of the present paper is to analyse the effect of a thin vertical rigid barrier over stepped bottom topography on reflection and transmission of incident water waves. This investigation helps in creating the calm zone near the seashore. Here, the problem is analysed using matched eigenfunction expansion method. The resulting system of equations is solved using algebraic least squares method. The performance of the barrier over step is studied through the graphs of reflection coefficient, transmission coefficient and non-dimensional horizontal force for various values of physical parameters.

2. Mathematical formulation

Let us assume the fluid under consideration is homogeneous, incompressible, inviscid and the fluid motion is irrotational and also simple harmonic in time t . The Cartesian coordinate system is taken with mean free surface along the xz -plane and y -axis is vertically downwards (taken as positive) through the thin vertical rigid barrier of length d over the step bottom topography (see Figure 1).

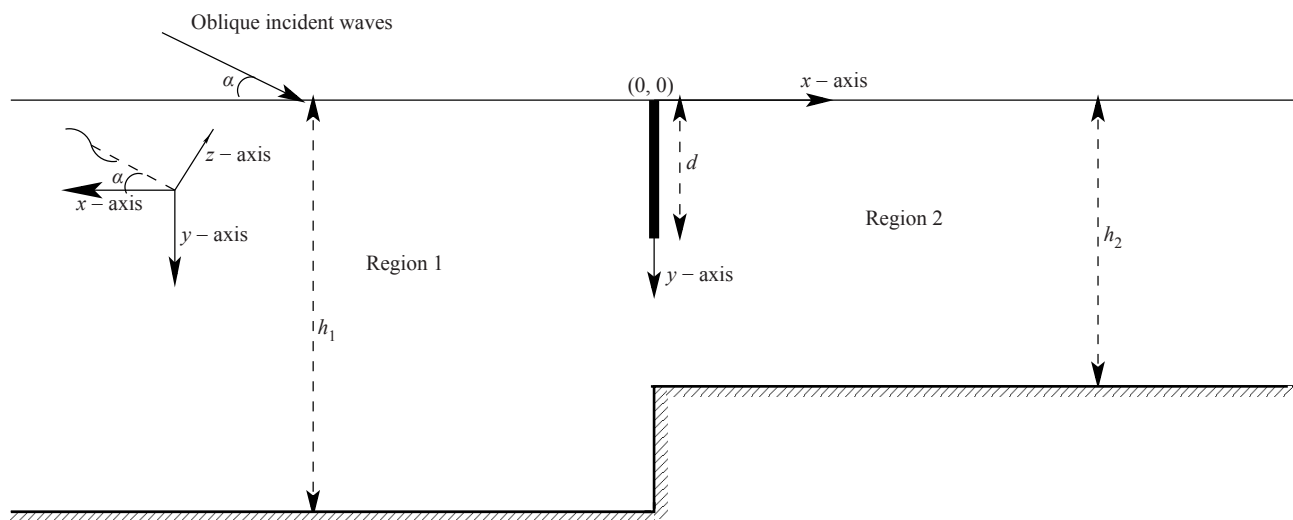


Figure 1. Schematic of the problem with rigid barrier over impermeable stepped bottom.

The position of the step is at $x = 0$, $h_2 \leq y \leq h_1$ and the barrier is at $x = 0$, $0 \leq y \leq d$. The fluid domain is divided into two regions such as $R_1 : -\infty < x \leq 0$, $0 \leq y \leq h_1$, $R_2 : 0 \leq x < \infty$, $0 \leq y \leq h_2$. Under the small amplitude theory of water waves, the velocity potential can be represented by $\Phi(x, y, z, t) = \Re \{ \phi(x, y) e^{i(\mu z - \omega t)} \}$, where \Re denotes the real part and ω is the angular frequency of the wave. The complex valued spatial potential $\phi(x, y)$ denoted as ϕ_1 for $x < 0$ and ϕ_2 for $x > 0$, satisfies the Helmholtz equation (Rhee [27])

$$\frac{\partial^2 \phi}{\partial x^2} + \frac{\partial^2 \phi}{\partial y^2} - \mu^2 \phi = 0 \text{ in the regions } R_j, j = 1, 2, \quad (1)$$

where $\mu = k_0 \sin \alpha$, α is the angle of incidence with respect to x -axis and k_0 is the wave number of the incident wave. Also, $\phi_j(x, y)$, $j = 1, 2$, satisfies the boundary conditions (Losada et al. [3] and Rhee [27]) as defined below:

$$\frac{\partial \phi_1}{\partial y} + K\phi_1 = 0 \text{ on } y = 0, -\infty < x < 0 \text{ (} K = \omega^2/g \text{)}, \quad (2)$$

$$\frac{\partial \phi_2}{\partial y} + K\phi_2 = 0 \text{ on } y = 0, 0 < x < \infty, \quad (3)$$

$$\frac{\partial \phi_1}{\partial y} = 0 \text{ on } y = h_1, -\infty < x < 0, \quad (4)$$

$$\frac{\partial \phi_2}{\partial y} = 0 \text{ on } y = h_2, 0 < x < \infty, \quad (5)$$

and the far-field conditions

$$\phi_1(x, y) \sim \frac{ig}{w} \{e^{is_0x} + Re^{-is_0x}\} \frac{\cosh k_0(y-h_1)}{\cosh k_0h_1} \text{ as } x \rightarrow -\infty, \quad (6)$$

and

$$\phi_2(x, y) \sim \frac{ig}{w} \{Te^{iq_0x}\} \frac{\cosh p_0(y-h_2)}{\cosh p_0h_2} \text{ as } x \rightarrow \infty, \quad (7)$$

where $s_0 = \sqrt{k_0^2 - \mu^2}$, $q_0 = \sqrt{p_0^2 - \mu^2}$; k_0 and p_0 satisfy the respective transcendental equations

$$k \tanh kh_1 - K = 0, \text{ and } k \tanh kh_2 - K = 0,$$

g is acceleration due to gravity and $|R|$ and $|T|$ respectively represent the reflection and transmission coefficients. Here, $\mu = k_0 \sin \alpha = p_0 \sin \beta$ due to the phase speed along the rays of the incident wave leading to Snell's law for refraction across the step at the bottom.

In addition to this, the matching conditions at $x = 0$ due to continuity of pressure and velocity are:

$$\phi_1(0, y) = \phi_2(0, y), d \leq y \leq h_2 \text{ (at the gap)}, \quad (8)$$

$$\frac{\partial \phi_1}{\partial x}(0, y) = \frac{\partial \phi_2}{\partial x}(0, y), d \leq y \leq h_2 \text{ (at the gap)}, \quad (9)$$

$$\frac{\partial \phi_1}{\partial x}(0, y) = \frac{\partial \phi_2}{\partial x}(0, y) = 0, 0 \leq y \leq d \text{ (at the barrier)}, \quad (10)$$

$$\frac{\partial \phi_1}{\partial x}(0, y) = 0, h_2 \leq y \leq h_1 \text{ (at the step)}. \quad (11)$$

The study uses the Eqs. (1)-(11) to coin a system of equations and the system of equations will be solved numerically to determine R and T which is described in the next section.

3. Method of solution

The Havelock's expansion for the velocity potential in regions R_j , $j = 1, 2$, are given by

$$\phi_1(x, y) = \frac{ig}{w} \left[\{e^{is_0x} + Re^{-is_0x}\} f_0(y) + \sum_{n=1}^{\infty} A_n e^{-is_nx} f_n(y) \right], \quad -\infty < x \leq 0, \quad 0 \leq y \leq h_1, \quad (12)$$

$$\phi_2(x, y) = \frac{ig}{w} \left[\{Te^{iq_0x}\} g_0(y) + \sum_{n=1}^{\infty} B_n e^{iq_nx} g_n(y) \right], \quad 0 \leq x < \infty, \quad 0 \leq y \leq h_2, \quad (13)$$

with $f_n(y) = \frac{\cosh k_n(y-h_1)}{\cosh k_n h_1}$, $g_n(y) = \frac{\cosh p_n(y-h_2)}{\cosh p_n h_2}$; $n = 0, 1, 2, \dots$ and k_n & p_n , $n = 0, 1, 2, \dots$ satisfy the transcendental equations $k \tanh kh_1 - K = 0$ and $p \tanh ph_2 - K = 0$ respectively. Here k_0, p_0 are real roots corresponding to propagating mode while k_n, p_n ($n = 1, 2, \dots$) are purely imaginary roots corresponding to evanescent modes. Also $s_n = \sqrt{k_n^2 - \mu^2}$, $q_n = \sqrt{p_n^2 - \mu^2}$ for $n = 1, 2, \dots$. The unknowns R, A_n, T, B_n , $n = 1, 2, 3, \dots$ are to be determined. After truncating the series to a finite number say N , we have $2N + 2$ number of unknowns.

Using the relations (12) and (13) in the conditions (8)-(11), we obtain

$$(1+R)f_0(y) + \sum_{n=1}^N A_n f_n(y) - Tg_0(y) - \sum_{n=1}^N B_n g_n(y) = 0, \quad d \leq y \leq h_2, \quad (14)$$

$$is_0(1-R)f_0(y) - \sum_{n=1}^N is_n A_n f_n(y) = 0, \quad 0 \leq y \leq d, \quad (15)$$

$$iq_0 Tg_0(y) + \sum_{n=1}^N iq_n B_n g_n(y) = 0, \quad 0 \leq y \leq d, \quad (16)$$

$$is_0(1-R)f_0(y) - \sum_{n=1}^N is_n A_n f_n(y) - iq_0 Tg_0(y) - \sum_{n=1}^N iq_n B_n g_n(y) = 0, \quad d \leq y \leq h_2, \quad (17)$$

$$is_0(1-R)f_0(y) - \sum_{n=1}^N is_n A_n f_n(y) = 0, \quad h_2 \leq y \leq h_1. \quad (18)$$

Approximate solution of the $2N + 2$ unknowns appearing in Eqs. (14)-(18) can be obtained by the method of algebraic least-squares for which we consider infinite number of discretized points: (i) $\hat{y}_1, \hat{y}_2, \hat{y}_3, \dots$ on the barrier (0, d), (ii) $\check{y}_1, \check{y}_2, \check{y}_3, \dots$ in the gap (d, h_2) and (iii) $\check{y}_1, \check{y}_2, \check{y}_3, \dots$ on the step (h_2, h_1), which lead to an overdetermined system with infinite number of equations in the matrix form as

$$A\vec{X} = \vec{b}, \quad (19)$$

where A is the coefficient matrix, \vec{b} is the known vector matrix and $\vec{X} = [R, A_n, T, B_n]$ ($n = 1, 2, 3, \dots, N$) is unknown vector matrix to be determined. The least square solution is found for which the following normal system need to be solved:

$$A^* A \bar{X} = A^* \bar{b}, \quad (20)$$

where A^* denotes the conjugate transpose of A . If A has linearly independent columns then the least-squares solution is unique and is given by

$$\bar{X} = (A^* A)^{-1} A^* \bar{b}. \quad (21)$$

Here, it may be noted that the ill-conditioned matrix can be avoided by choosing the appropriate discretized points (see Section 5). The non-dimensional horizontal force per unit width of the barrier over the step-type bottom is given by

$$\frac{|F_h|}{\rho g h_1 A} = \frac{\omega}{g h_1} \left| \int_0^d (\phi_2(0, y) - \phi_1(0, y)) dy \right|. \quad (22)$$

4. Energy balance relation

The energy identity relating to reflection and transmission coefficients of the given problem, can be derived by using Green's integral theorem:

$$\int_{\Gamma} \left(\phi \frac{\partial \phi^*}{\partial n} - \phi^* \frac{\partial \phi}{\partial n} \right) dS = 0, \quad (23)$$

where $\frac{\partial}{\partial n}$ is the outward normal derivative to the boundary Γ , ϕ^* is the complex conjugate of ϕ , Γ is composed of $\{-X \leq x \leq 0, y = 0\} \cup \{x = -X, 0 \leq y \leq h_1\} \cup \{-X \leq x \leq 0, y = h_1\} \cup \{x = 0, h_2 \leq y \leq h_1\} \cup \{0 \leq x \leq X, 0 \leq y \leq h_2\} \cup \{x = X, 0 \leq y \leq h_2\} \cup \{0 \leq x \leq X, y = 0\} \cup \{x = 0^+, 0 \leq y \leq d\} \cup \{x = 0^-, 0 \leq y \leq d\}$ and then we take $X \rightarrow \infty$.

The contribution to the integral (23) is zero due to the bottom as well as the barrier since $\frac{\partial \phi}{\partial n} = 0$ & $\frac{\partial \phi^*}{\partial n} = 0$. The contribution to the integral (23) at the free surface is zero. The contribution from the line $x = -X, 0 \leq y \leq h_1$ is

$$\int_0^{h_1} \left(\phi_1 \frac{\partial \phi_1^*}{\partial x} - \phi_1^* \frac{\partial \phi_1}{\partial x} \right) dy = \frac{g^2}{\omega^2} \frac{is_0 (|R|^2 - 1)}{2k_0 \cosh^2(k_0 h_1)} [2k_0 h_1 + \sinh(2k_0 h_1)]. \quad (24)$$

At the line $x = X, 0 \leq y \leq h_2$, the integral gives rise to

$$\int_{h_2}^0 \left(\phi_2 \frac{\partial \phi_2^*}{\partial x} - \phi_2^* \frac{\partial \phi_2}{\partial x} \right) dy = \frac{g^2}{\omega^2} \frac{iq_0 |T|^2}{2p_0 \cosh^2(p_0 h_2)} [2p_0 h_2 + \sinh(2p_0 h_2)]. \quad (25)$$

On adding all of these contributions in Eq. (23), we get the energy identity as

$$|R|^2 + \delta |T|^2 = 1, \quad (26)$$

where $\delta = \frac{iq_0 k_0 (2p_0 h_2 + \sinh(2p_0 h_2)) \cosh^2(k_0 h_1)}{is_0 p_0 (2k_0 h_1 + \sinh(2k_0 h_1)) \cosh^2(p_0 h_2)}$.

5. Numerical results

Here, the reflection coefficient $|R|$ and transmission coefficient $|T|$ are computed by solving the system given in Eq. (19) using algebraic least-squares method. The non-dimensional horizontal force on the barrier is computed numerically from the Eq. (22). These values are shown through tables and also through graphs for various values of parameters. For applying the algebraic least-square method, we consider different number of equally spaced discretized points, say m_1 points on the barrier: $\hat{y}_i = id/(m_1 - 1)$, $i = 0, 1, 2, \dots, (m_1 - 1)$, m_2 points in the gap: $\hat{y}_i = d + i(h_2 - d)/(m_2 - 1)$, $i = 0, 1, 2, \dots, (m_2 - 1)$ and m_3 points on the step: $\hat{y}_i = h_2 + i(h_1 - h_2)/(m_3 - 1)$, $i = 0, 1, 2, \dots, (m_3 - 1)$. Thus, from Eqs. (14)-(18), we obtain $2(m_1 + m_2) + m_3 = \hat{m}$ (say) equations in $2N + 2$ unknowns which are to be determined by solving the system (19). The non-dimensionalization of the physical parameters is made using both the depths h_1 & h_2 . Here, the non-dimensional parameter are d/h_1 , Kh_1 , $H = h_2/h_1$, $p_0 h_2$.

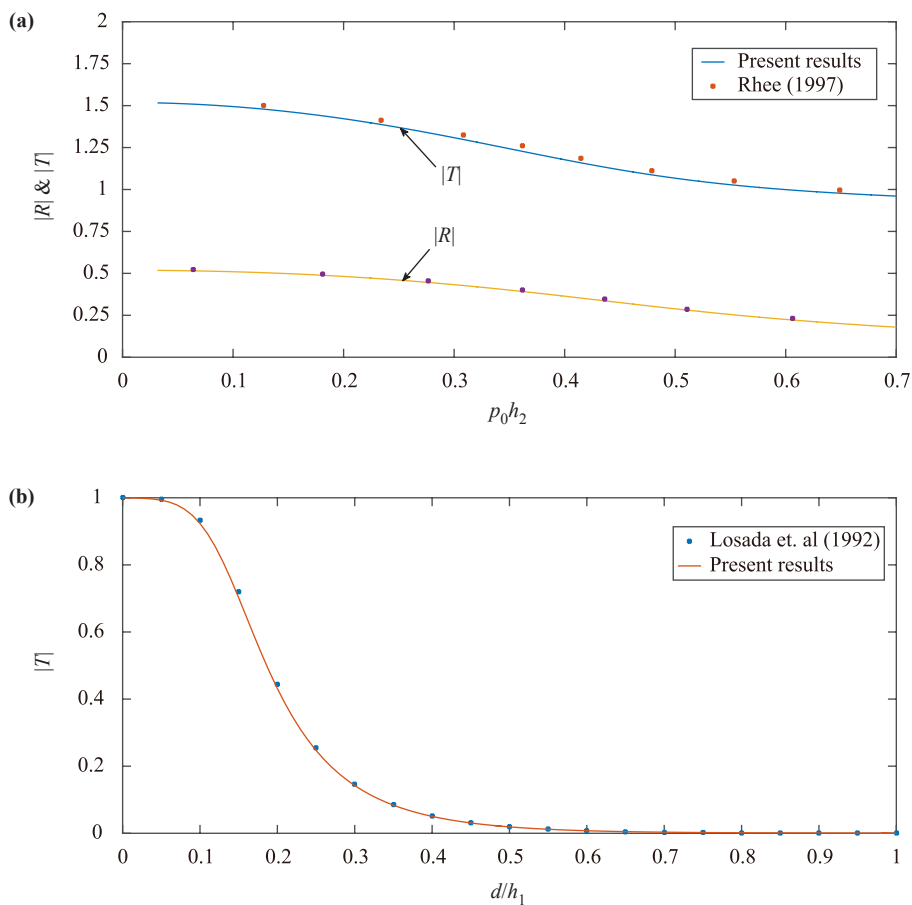


Figure 2. Comparison of the present results with (a) Rhee [27] with $H = 0.1$, $\alpha = 0$, $d/h_1 = 0$ (b) Losada et al. (1992) with $H = 1.0$, $Kh_1 = 4.262$, $\alpha = 0$.

5.1 Validation

For validation of the present results, the results for absence of barrier and presence of vertical step h_2/h_1 , are compared with results of Rhee [27] in Figure 2(a). Here, $|R|$ and $|T|$ against $p_0 h_2$ are drawn where the present results (solid lines) fully coincide with Rhee [27] (stars), proving the correctness of present results. In Figure 2(b), the present results for $|T|$ are compared with Losada et al. [3] for vertical barrier over flat bed (in the absence of step). The transmission coefficient $|T|$ against the dimensionless barrier length d/h_1 for fixed $Kh_1 = 4.262$ and $\alpha = 0$ is presented in Figure 2(b)

where the present results agree well with those of Losada et al. [3]. This proves the correctness of the present results. In Table 1, $|R|$ and $|T|$ are calculated for different non-dimensional values of Kh_1 and the results tabulated here show that the current numerical results verify the energy balance relation (26) showing again the correctness of the present results.

Table 1. Energy identity verification for $d/h_1 = 0.6, H = 0.9, \alpha = \pi/4$.

Kh_1	$ R $	$ T $	$ R ^2 + \gamma T ^2$
0.5	0.2836709	0.971339	0.998969
1	0.542422	0.839165	0.996779
1.5	0.797381	0.595626	0.995996
2	0.938224	0.339009	0.997709
2.5	0.984274	0.172273	0.999051
3	0.996101	0.085408	0.999610
3.5	0.998994	0.042712	0.999828
4	0.999722	0.021717	0.999918
4.5	0.999916	0.011221	0.999959

5.2 Convergence for N and (m_1, m_2, m_3)

The convergence of N (the number of evanescent modes) and the convergence of number of discretization points (m_1, m_2, m_3) are examined. In Table 2, the values of $|R|$ are given versus Kh_1 for various values of $N = 10, 20, 30, 55$ and 60 for fixed values of $d/h_1 = 0.6, H = 0.9, \alpha = \pi/4$. The tabular data show that the accuracy in $|R|$ upto two decimal places are obtained with $N = 55$ for all the values of Kh_1 . Further, the Table 3 shows the tabulated values of $|R|$ and $|T|$ versus Kh_1 for various values of (m_1, m_2, m_3) for fixed values of $d/h_1 = 0.3, H = 0.5, \alpha = 0$ and $N = 55$. The tabular data show that the accuracy in the results upto four decimal places are obtained with $(m_1, m_2, m_3) = (700, 700, 350)$.

Table 2. $|R|$ versus Kh_1 for various values of $N = 10, 20, 30, 55$ and 60 .

Kh_1	$ R (N = 10)$	$ R (N = 20)$	$ R (N = 30)$	$ R (N = 55)$	$ R (N = 60)$
0.5	0.301273	0.294279	0.289798	0.284316	0.283670
1	0.564326	0.556549	0.550659	0.543309	0.542421
1.5	0.810078	0.806768	0.802992	0.798008	0.797381
2	0.940626	0.941080	0.940057	0.938443	0.938224
2.5	0.983528	0.984619	0.984594	0.984321	0.984273
3	0.995167	0.995944	0.996081	0.996105	0.996100

Table 3. $|R|$ and $|T|$ versus Kh_1 for fixed $N = 55$ with different values of (m_1, m_2, m_3) .

Kh_1	(m_1, m_2, m_3)	$ R $	$ T $
0.1	(100,100,50)	0.197766	1.151433
	(200,200,100)	0.197685	1.151281
	(400,400,200)	0.197632	1.151208
	(700,700,350)	0.197599	1.151172
	(800,800,400)	0.197588	1.151156
0.5	(100,100,50)	0.294316	1.064908
	(200,200,100)	0.294429	1.064789
	(400,400,200)	0.294445	1.064757
	(700,700,350)	0.294438	1.064742
	(800,800,400)	0.294434	1.064736
0.7	(100,100,50)	0.342612	1.019294
	(200,200,100)	0.342789	1.019196
	(400,400,200)	0.342826	1.019186
	(700,700,350)	0.342827	1.019182
	(800,800,400)	0.342826	1.019180

5.3 Influence of physical parameters on the reflection coefficient, transmission coefficient and force on the barrier over stepped bottom

Here, the reflection $|R|$ and transmission $|T|$ coefficients, and the force on the barrier are calculated numerically and plotted through different graphs for various values of the parameters.

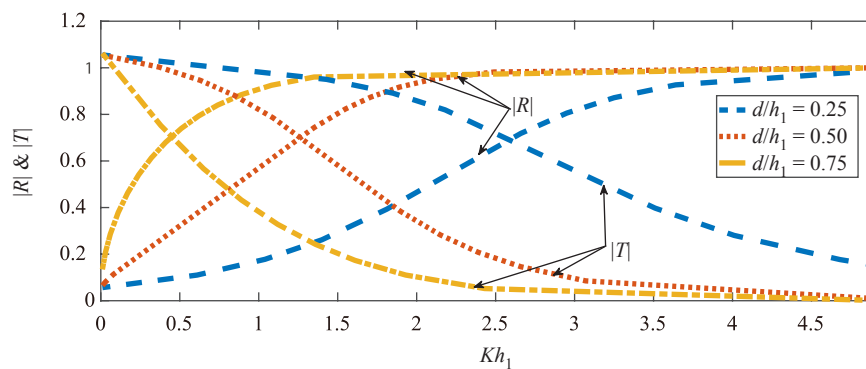


Figure 3. $|R|$ and $|T|$ varying against Kh_1 for $H = 0.8$ and $\alpha = 0$ with different barrier length.

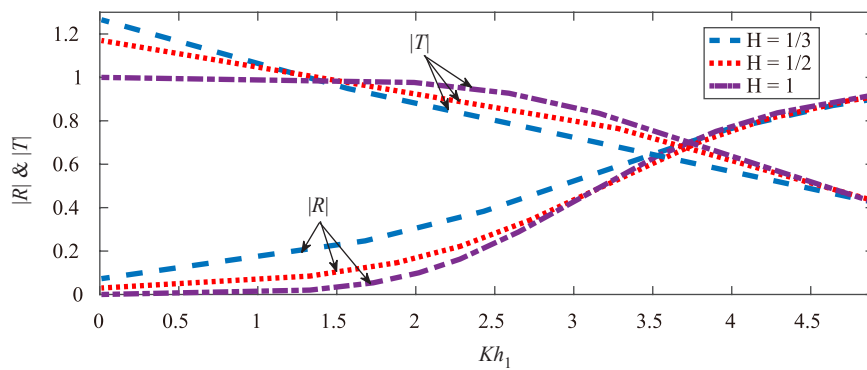


Figure 4. $|R|$ and $|T|$ varying against Kh_1 for $d/h_1=0.2$ and $\alpha = \pi/4$ with different H .

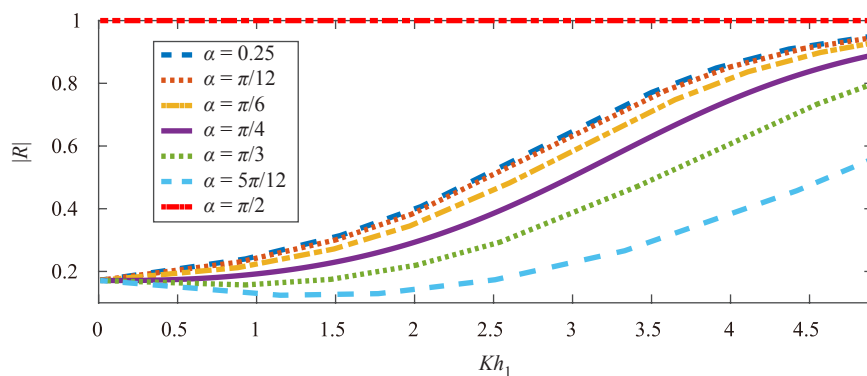


Figure 5. $|R|$ versus Kh_1 for $d/h_1=0.2$ and $H = 0.5$ with different α .

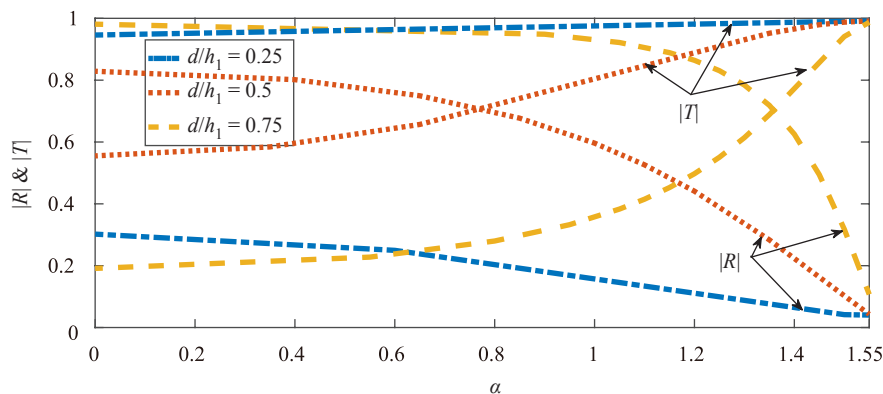


Figure 6. $|R|$ and $|T|$ versus α for $Kh_1 = 1.5$ and $H = 0.8$ with different length of the barrier.

The variation of $|R|$ & $|T|$ against the non-dimensional wave frequency Kh_1 for three different lengths of the barrier is shown in Figure 3. It is observed that the reflection coefficient increases as the length of the barrier d/h_1 increases from 0.25 to 0.75. Consequently, the transmission co-efficient decreases as the length of the barrier increases. Also, the reflection coefficient increases while transmission coefficient decreases as the non-dimensional wave frequency increases. Hence, larger frequency waves gets maximum reflection and minimum transmission. This may happen due to

the fact that larger frequency waves almost confined near the free surface and hence gets comparatively more reflection and lesser transmission. In Figure 4, the variation of reflection $|R|$ and transmission $|T|$ coefficients as a function of non-dimensional wave frequency Kh_1 for three different step heights at the bottom is reported. The reflection coefficient $|R|$ decreases while transmission coefficient $|T|$ increases as the depth ratio H increases (i.e. the step height decreases). The effect of depth ratio H on $|R|$ & $|T|$ is diminished as the value of Kh_1 becomes larger which may be due to the fact that the larger frequency waves i.e. waves with short wavelength are almost confined near the free surface and get lesser influenced due to the stepped bottom. It is also noticed that the pattern of transmission coefficient is also different for $Kh_1 < 1$, which may be due to phase shift in transmitted waves by altering depth ratio. Figure 5 shows $|R|$ versus Kh_1 for different values of angle of incidence. As the angle of incidence α increases, the reflection coefficient decreases. Also, there is more reflection for normal incidence case ($\alpha = 0$) in comparison to oblique incidence case. It is also observed that $|R|$ becomes unity for $\alpha = \pi/2$ for all the frequencies of incident waves, which validate the physical behaviour of the problem. In Figure 6, $|R|$ and $|T|$ versus angle of incidence α for different barrier length are plotted. The reflection coefficient monotonically decreases with the angle of incidence for all these dimensionless lengths of the barrier ranging from 0.25 – 0.75. This is due to the fact that the only x-component of the incident wave is reflected by the present barrier and becomes smaller with the increase of angle of incidence. Consequently, the transmission coefficient monotonically increases with the angle of incidence for all these dimensionless lengths of the barrier.

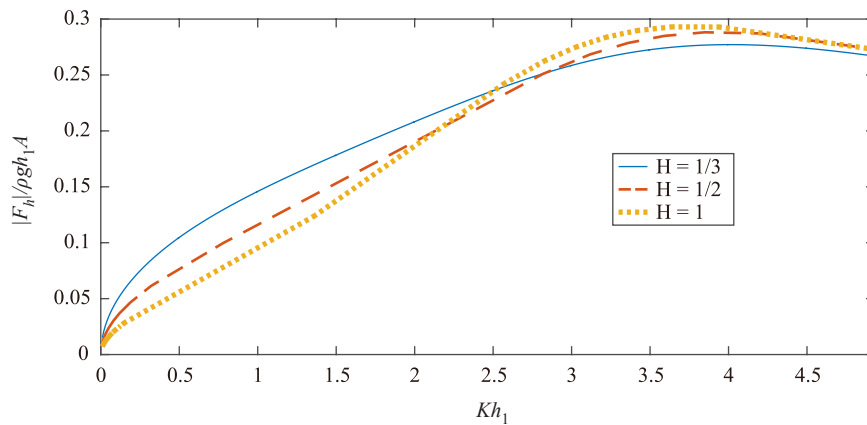


Figure 7. Dimensionless force varying against Kh_1 for $d/h_1 = 0.3$ and $\alpha = 0$ with different depth ratio H .

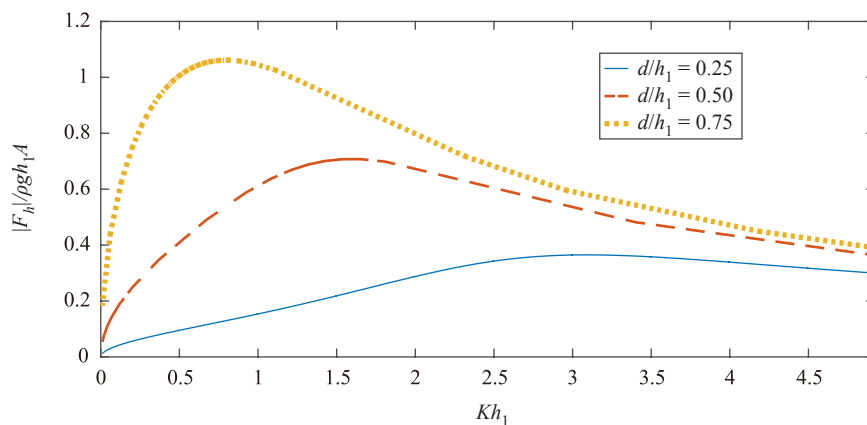


Figure 8. Dimensionless force varying against Kh_1 for $H = 0.8$ and $\alpha = 0$ with different barrier lengths.

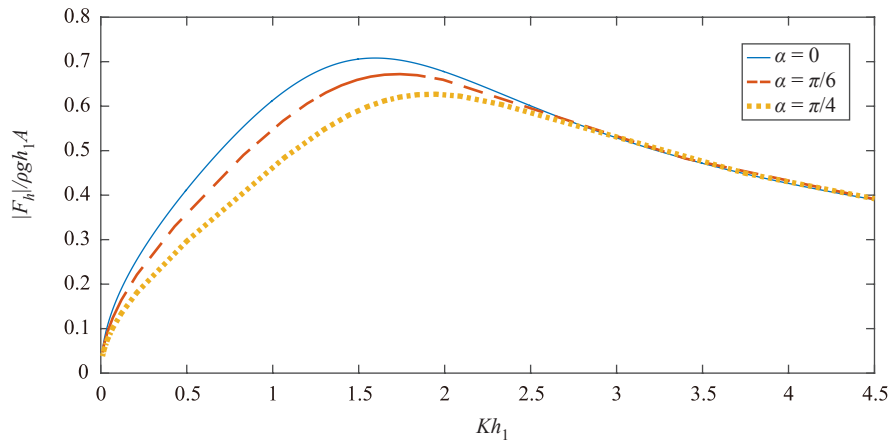


Figure 9. Dimensionless force versus Kh_1 for $d/h_1 = 0.4$ and $H = 0.8$ with different α .

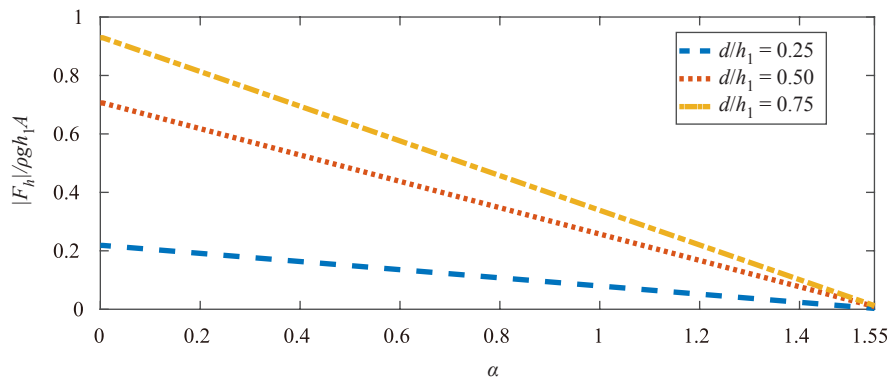


Figure 10. Dimensionless force versus α for $Kh_1 = 1.5$ and $H = 0.8$ with different length of the barrier.

The variation of the non-dimensional horizontal force $|F_h|/\rho gh_1 A$ against the non-dimensional wave frequency Kh_1 is reported in Figure 7. For $Kh_1 < 2.5$, the force on the barrier decreases as H increases while for $Kh_1 > 2.5$, the force on the barrier increases as H increases. The pattern in the curves in Figure 7 is changing because there may be a phase shift due to alteration of depth ratio for each curve. In Figure 8, the variation of $|F_h|/\rho gh_1 A$ as a function of Kh_1 is shown for three different lengths of the barrier $d/h_1 = 0.25, 0.50, 0.75$. It is observed that the force on the barrier increases as the value of d/h_1 increases which is similar to the observations obtained in Figure 3 for reflection curves. Figure 9 shows the non-dimensional horizontal force versus Kh_1 for three different angle of incidence $\alpha = 0, \pi/6, \pi/4$. The maximum value of the non-dimensional horizontal force on the barrier decreases as the angle incidence increases. In Figure 10, the non-dimensional horizontal force versus angle of incidence α for three different dimensionless lengths of the barrier ranging from 0.25 – 0.75 is demonstrated. It is observed that the dimensionless force decreases versus angle of incidence for each dimensionless lengths of the barrier. This observation is similar to reflection curves of Figure 6.

6. Conclusions

In the present work, an oblique surface wave scattering by thin vertical rigid barrier over a step bottom topography is examined for its solution using matched eigenfunction expansion method by the aid of algebraic least squares method. The performance of the barrier over step is studied through various graphs of the reflection and transmission coefficients

and non-dimensional horizontal force. The reflection coefficient increases as the length of the barrier and the step height increase while it decreases as the angle of incidence increases. Also, the maximum reflection occurs for normal incidence of the incident waves. The analysis of non-dimensional horizontal force per unit width of the barrier is also examined. As the length of the barrier over the step increases, the peak on force curves goes up. The non-dimensional horizontal force and reflection decrease as the angle of incidence increases for a fixed barrier length, which is due to the fact that the only x-component of the incident wave is reflected by the present barrier and becomes smaller with the increase of angle of incidence. Also, it is noticed that the force on the barrier is less for obliquely incidence waves in comparison of normal incidence waves. These results conclude that the barrier along with step works as an effective barrier to reflect more incident waves causing calm zone along lee side, yielding less impact on seashore.

Conflict of interest

The authors declare no conflicts of interest.

References

- [1] Bai KJ. Diffraction of oblique waves by an infinite cylinder. *Journal of Fluid Mechanics*. 1975; 68(3): 513-535. Available from: <https://doi.org/10.1017/S0022112075001802>.
- [2] Evans DV. Diffraction of water waves by a submerged vertical plate. *Journal of Fluid Mechanics*. 1970; 40(3): 433-451. Available from: <https://doi.org/10.1017/S0022112070000253>.
- [3] Losada IJ, Losada MA, Roldan AJ. Propagation of oblique incident waves past rigid vertical thin barriers. *Applied Ocean Research*. 1992; 14: 191-199. Available from: [https://doi.org/10.1016/0141-1187\(92\)90014-B](https://doi.org/10.1016/0141-1187(92)90014-B).
- [4] Porter R, Evans DV. Complementary approximations to wave scattering by vertical barriers. *Journal of Fluid Mechanics*. 1995; 294: 155-180. Available from: <https://doi.org/10.1017/S0022112095002849>.
- [5] Gayen R, Mondal A. A hypersingular integral equation approach to the porous plate problem. *Applied Ocean Research*. 2014; 46: 70-78. Available from: <https://doi.org/10.1016/j.apor.2014.01.006>.
- [6] Chakraborty R, Mandal BN. Water wave scattering by a rectangular submarine trench. *Journal of Engineering Mathematics*. 2014; 89(1): 101-112. Available from: <https://doi.org/10.1007/s10665-014-9705-6>.
- [7] Chakraborty R, Mandal BN. Oblique wave scattering by a rectangular submarine trench. *The ANZIAM Journal*. 2015; 56(3): 286-298. Available from: <https://doi.org/10.21914/anziamj.v56i0.7922>.
- [8] Tseng I-F; You C-S; Tsai C-C. Bragg reflections of oblique water waves by periodic surface piercing and submerged breakwaters. *Journal of Marine Science and Engineering*. 2020; 8(7): 522. Available from: <https://doi.org/10.3390/jmse8070522>.
- [9] Tran C-T, Chang J-Y, Tsai C-C. Step approximation for water wave scattering by multiple thin barriers over undulated bottoms. *Journal of Marine Science and Engineering*. 2021; 9(6): 629. Available from: <https://doi.org/10.3390/jmse9060629>.
- [10] Borah P, Hassan M. Wave loads by an oscillating water column in presence of bottom-mounted obstacle in the channel of finite depth. *SN Applied Sciences*. 2019; 1(10): 1-8. Available from: <https://doi.org/10.1007/s42452-019-1265-y>.
- [11] Koley S, Behera H, Sahoo T. Oblique wave trapping by porous structures near a wall. *Journal of Engineering Mathematics*. 2015; 141(3): 04014122.
- [12] Panduranga K, Koley S, Sahoo T. Surface gravity wave scattering by multiple slatted screens placed near a caisson porous breakwater in the presence of seabed undulations. *Applied Ocean Research*. 2021; 111: 102675.
- [13] Das S, Bora SN. Reflection of oblique ocean water waves by a vertical porous structure placed on a multi-step impermeable bottom. *Applied Ocean Research*. 2014; 47: 373-385. Available from: <https://doi.org/10.1016/j.apor.2014.07.001>.
- [14] Meng QR, Lu DQ. Scattering of gravity waves by a porous rectangular barrier on a seabed. *Journal of Hydrodynamics, Ser. B*. 2016; 28(3): 519-522. Available from: [https://doi.org/10.1016/S1001-6058\(16\)60656-X](https://doi.org/10.1016/S1001-6058(16)60656-X).
- [15] Kaligatla RB, Prasad NM, Tabssum S. Oblique interaction between water waves and a partially submerged rectangular breakwater. *Journal of Engineering for the Maritime Environment*. 2020; 234(1): 154-169. Available from: <https://doi.org/10.1177/14750902198537>.

- [16] Ray S, De S, Mandal BN. Wave propagation over a rectangular trench in the presence of a partially immersed barrier. *Fluid Dynamics Research*. 2021; 53(3): 035509. Available from: <https://doi.org/10.1088/1873-7005/ac0a93>.
- [17] Liu H-W, Zeng H-D, Huang H-D. Bragg resonant reflection of surface waves from deep water to shallow water by a finite array of trapezoidal bars. *Applied Ocean Research*. 2020; 94: 101976. Available from: <https://doi.org/10.1016/j.apor.2019.101976>.
- [18] Ni Y-L, Teng B. Bragg resonant reflection of water waves by a Bragg breakwater with porous trapezoidal bars on a sloping permeable seabed. *Applied Ocean Research*. 2021; 114: 102770. Available from: <https://doi.org/10.1016/j.apor.2021.102770>.
- [19] Singh S, Singh AK, Guha S. Reflection of plane waves at the stress-free/rigid surface of a micro-mechanically modeled Piezo-electro-magnetic fiber-reinforced half-space. *Waves in Random and Complex Media*. 2022; 32: 1-30.
- [20] Singh AK, Mahto S, Guha S. Analysis of plane wave reflection phenomenon from the surface of a micro-mechanically modeled piezomagnetic fiber-reinforced composite half-space. *Waves in Random and Complex Media*. 2021; 31: 1-22.
- [21] Bhatti MM, Lu DQ. Head-on collision between two hydroelastic solitary waves in shallow water. *Qualitative Theory of Dynamical Systems*. 2018; 17(1): 103-122.
- [22] Guo Y, Liu Y, Meng X. Oblique wave scattering by a semi-infinite elastic plate with finite draft floating on a step topography. *Acta Oceanologica Sinica*. 2016; 35(7): 113-121.
- [23] Venkateswarlu V, Karmakar D. Influence of impermeable elevated bottom on the wave scattering due to multiple porous structure. *Applied Fluid Mechanics*. 2020; 13(1): 371-385.
- [24] Dhillon H, Banerjee S, Mandal BN. Water wave scattering by a finite dock over a step-type bottom topography. *Ocean Engineering*. 2016; 113: 1-10. Available from: <https://doi.org/10.1016/j.oceaneng.2015.12.017>.
- [25] Praveen KM, Venkateswarlu V, Karmakar D. Wave transformation due to finite elastic plate with abrupt change in bottom topography. *Ships and Offshore Structures*. 2021; 17(8): 1-19. Available from: <https://doi.org/10.1080/17445302.2021.1946308>.
- [26] Vijay KG, Venkateswarlu V, Sahoo T. Bragg scattering of surface gravity waves by an array of submerged breakwaters and a floating dock. *Wave Motion*. 2021; 106: 1-20.
- [27] Rhee JP. On the transmission of water waves over a shelf. *Applied Ocean Research*. 1997; 19: 161-167.
- [28] Guha S, Singh AK. Plane wave reflection/transmission in imperfectly bonded initially stressed rotating piezothermoelastic fiber-reinforced composite half-spaces. *European Journal of Mechanics-A/Solids*. 2021; 88: 104242.